EPJ Web of Conferences **60**, 19006 (2013)
DOI: 10.1051/epjconf/20136019006

W and Z boson production at CMS

Francesco Romeo[1, a]

[1] *Università degli Studi di Perugia*

Abstract. We present selected measurements regarding W and Z bosons performed with the CMS detector, based on samples of events collected during 2011 and 2012 LHC physics runs. Measurements include W and Z inclusive cross sections, transverse momentum distribution with Z events, Drell-Yan differential and double-differential cross sections, and lepton charge asymmetry in W events.

1 Introduction

Theoretical predictions in the Standard Model of particle physics (SM) can be done at next-to-leading order (NLO) and at next-to-next-to-leading order (NNLO) [1], [2] in perturbative QCD and programs like POWHEG, or FEWZ, RESBOS provide full event generation at these two oder respectively. The calculations are mainly limited by uncertainties on parton distribution functions (PDFs), higher-order QCD, and electroweak (EWK) radiative corrections.

W and Z bosons produced at the high energy proton-proton collisions of LHC have a clean signature and give the possibility to perform precision measurements. The study of their properties is therefore an important test of the SM predictions and can provide significant contributions to PDFs.

In this sense measurements of inclusive, differential and double differential cross sections are of particular interest. Distribution in rapidity, Υ, directly reflects the PDFs of the interacting partons. The rapidity of the Drell-Yan dilepton produced in proton-proton collisions is related to the momentum fraction $x_+(x_-)$ carried by the parton in the forward-going (backward-going) proton as described by the leading-order formula $x_\pm = \frac{M}{\sqrt{s}} e^{\pm\Upsilon}$. A measurement of W charge asymmetry as a function of boson rapidity can provide new insights on the u/d ratio and the sea antiquark densities.

Events containing W and Z moreover are themselves useful tools to understand and calibrate the detector. The tag-and-proble (T&P) method is extensively used to determine lepton efficiencies from high-purity samples of $Z \rightarrow l^+l^-$ events, which are also used to study lepton momentum scale and resolution. Finally many searches for new physics have electroweak processes among their main backgrounds, hence studying electroweak processes is also important to keep backgrounds to such searches under control.

a. e-mail: fromeo@cern.ch

2 W and Z boson measurements

The following measurements will be discussed in detail in the sections below : inclusive W and Z boson cross sections at $\sqrt{s} = 8$ TeV [3], measurement of the transverse momentum distribution of Z bosons decaying to dimuons at $\sqrt{s} = 8$ TeV [4], measurement of the differential and double-differential Drell-Yan cross sections at $\sqrt{s} = 7$ TeV [5], measurement of lepton charge asymmetry at $\sqrt{s} = 7$ TeV [6], [7].

In order to perform precision measurements of the inclusive W and Z boson cross sections and transverse momentum distribution of Z bosons decaying to dimuons at $\sqrt{s} = 8$ TeV, a dedicated LHC configuration was deployed to accumulate a dataset with low pileup and low transverse momentum trigger thresholds. The basic idea is simple and consists of reducing the instantaneous luminosity, and by the same proportion the pileup, by separating the LHC beams in the transverse plane to diminish the effective overlap. The working point was chosen to allow manageable rates with an unprescaled single lepton trigger with sufficiently loose requirements, and at the same time yielding a low average pileup. The corresponding instantaneous luminosity ranged from 3×10^{32} to 6×10^{32} $cm^{-2}s^{-1}$. The separation of the beam during the data taking was periodically adjusted to compensate the natural loss of instantaneous luminosity ("leveling"). The total integrated luminosity is 18.7 pb^{-1} for W and Z inclusive cross-section and 18.4 pb^{-1} for the measurement of the transverse momentum distribution of Z bosons decaying to dimuons.

The measurement of the differential and double-differential Drell-Yan cross sections are based on data recorded in 2011 at $\sqrt{s} = 7$ TeV, corresponding to an integrated luminosity of 4.5 fb^{-1} and 4.8 fb^{-1} for dimuon and dielectron channels respectively. Lepton charge asymmetry is also performed with data taken in 2011 at $\sqrt{s} = 7$ TeV, with and integrated luminosity of 840 pb^{-1} for $W \rightarrow e\nu$ and 234 pb^{-1} for $W \rightarrow \mu\nu$.

All measurements have been done with the CMS detector [8] and make use of two main objects : e[9], μ[10].

3 Inclusive W and Z boson cross sections at $\sqrt{s}$ = 8 TeV

3.1 Analysis strategy

The online selection of W and Z boson events is based on single electron and muon triggers with thresholds of 22 GeV and 15 GeV, respectively, at the high level trigger. Electrons are required to have $E_T > 25$ GeV and to be within $|\eta| < 1.4442$ (barrel) or $1.566 < |\eta| < 2.5$ (endcap), skipping the transition region between barrel and endcap. Muons must have pT > 25 GeV and $\eta < 2.1$. The electron and muon efficiencies are estimated in simulation and then corrected by the differences between data and simulation using the $T\&P$ technique. Leptonic W boson decays are characterized by a prompt, energetic, and isolated lepton and a neutrino giving rise to significant missing transverse energy, E_T^{miss}. The Z boson Drell-Yan decays are selected based on two energetic and isolated leptons. The reconstructed dilepton mass is used to estimate efficiencies and measure event yields.

The acceptance, A, for W or Z boson events is defined as the fraction of simulated events having the boson decay products within the fiducial volume and satisfying event selection. For Z events, considerations are restricted to events with generated boson mass between 60 GeV and 120 GeV.

The signal and background yields are obtained by fitting the E_T^{miss} distributions for $W \to e\nu$ and $W \to \mu\nu$ to different functional models. An accurate E_T^{miss} measurement is essential for distinguishing a W signal from QCD multijet backgrounds. Drell-Yan lepton pair, that can be a background when one of the two lepton disappears into a non-fiducial region, are suppressed vetoing events with two reconstructed leptons. $W \to \tau\nu$ and $Z \to \tau\tau$ can be reduced asking high pT of leptons. Top quark pair and dibosons (WW, WZ, ZZ) backgrounds are quite small. Selected events are fitted as a sum of 3 contributions with the formula :

$$af1 + bf2 + cf3$$

$f1$ is the MC histogram template defined using boson recoil corrected from data and used to extract signal. $f2$ is a parametric function (modified Rayleigh distribution) to model the QCD background :

$$f_{QCD}(E_T^{miss}) = E_T^{miss} exp(-\frac{E_T^{miss2}}{2(\sigma_0+\sigma_1 E_T^{miss})^2})$$

$f3$ is histogram template derived from MC simultation to account for other EWK backgrounds. The EWK contributions are normalized to the W signal yield in the fit through the ratios of the theoretical cross sections, so that $c = \sigma(EWK)/\sigma(W) * a$. a, b represente the W and QCD signal yield respectively and together with σ_0, σ_1 are the free parameters of the binned maximum likelihood fit to the E_T^{miss} distribution. To extract the Z boson yield, the events in the Z mass peak are counted. Table 1 summarize all systematic uncertainties and the total uncertainty on the measurement for the electron and muon channel.

Table 1. Systematic uncertainties in percent for the electron and muon channel. "-" means that the source does not apply or is negligible.

Source	W^+		W^-		W		Z	
	e	μ	e	μ	e	μ	e	μ
Lepton reco & ID	2.8	1.0	2.5	0.9	2.5	1.0	2.8	1.1
Mom scale & res	0.4	0.3	0.7	0.3	0.5	0.3	-	-
E_T^{miss} scale & res	0.8	0.5	0.7	0.5	0.8	0.5	-	-
Bkg sub/mod	0.2	0.2	0.3	0.1	0.3	0.1	0.4	0.4
Total exp	3.0	1.2	2.7	1.1	2.7	1.2	2.8	1.2
Th uncertainty	2.1	2.0	2.6	2.5	2.7	2.2	2.6	1.9
Lumi	4.4	4.4	4.4	4.4	4.4	4.4	4.4	4.4
Total	5.7	5.0	5.8	5.2	5.8	5.1	5.8	4.9

3.2 Results

The results for the electron and muon channels are presented separately and are combined by calculating an average value weighted by the statistical and systematic uncertainties summed taking into account the correlated uncertainties that are only numerically relevant for theoretical uncertainties. The theoretical predictions of cross sections quoted in this section are computed at NNLO with the program FEWZ and the MSTW2008 set of PDFs. Summaries of the measurements are given in fig. 1 illustrating the consistency of the measurements in the electron and muon channels, as well as confirming the theoretical predictions. The statistical error is represented in black and the total experimental uncertainty, obtained by adding in quadrature the statistical and systematic uncertainties, is in red. For the cross section measurements, the luminosity uncertainty is added to the experimental uncertainty, and is represented in green. The yellow vertical line represents the theoretical prediction, and the light-yellow vertical band is the theoretical uncertainty, interpreted as a 68% confidence interval. In all cases there is a good agreement of

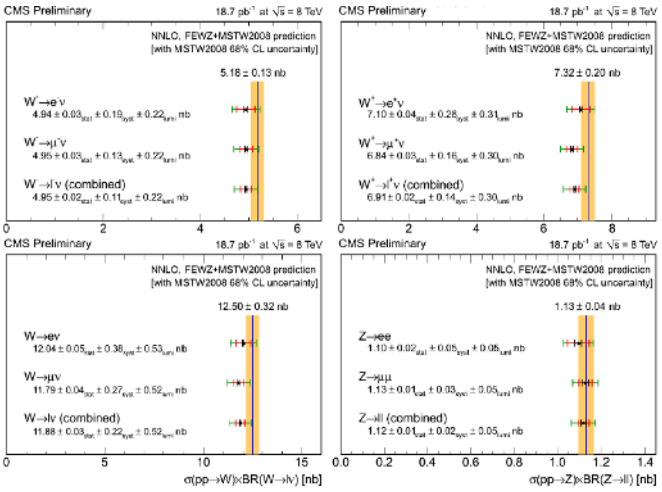

Figure 1. Summary of the W and Z production cross section times branching ratio measurements.

measured values with NNLO predictions.

4 Measurement of the transverse momentum distribution of Z bosons decaying to dimuons at $\sqrt{s}$ = 8 TeV

4.1 Analysis strategy

Events used in the analysis were collected with a single-muon trigger which requires the presence of at least one muon with qT greater than 15 GeV and $|\eta| < 2.1$. Offline inclusive dimuon candidates are selected requiring both muons to have qT > 20 GeV and $|\eta| < 2.1$. Each of the two muons is required to be sufficiently isolated from the other charged particles. Finally the muon pair is required to have a reconstructed invariant mass in the range between 60 to 120 GeV, to be consistent with the decay of the Z boson.

The differential cross section is determined in each qT bin by subtracting the estimated number of background events from the total number of detected events in a bin. The main sources of background, which could mimic the dileptons, are $Z \to \tau\tau$, $t\bar{t}$, W + jets, and diboson (WW, WZ and ZZ) productions with the subsequent decays of W, Z and τ via muons. The background events from the $Z \to \tau\tau$, $t\bar{t}$, and diboson processes are flavour symmetric and produce twice as many $e\mu$ pairs as ee or $\mu\mu$ pairs. Hence, these background contributions, evaluated from MC, could be additionally cross-checked with data, by analyzing the qT spectrum of the $e\mu$ pairs in the final state. After all the selections, the total background contamination is estimated to less than 1%,

The individual muon detection and selection efficiencies are determined with the $T\&P$ method.

The bin widths in qT distribution, which varies from 2.5 to 350 GeV, are chosen to provide sufficient resolution to observe the shape of the distribution, to limit migration of events between the bins, as well as to ensure sufficient number of events in each bin.

The measured qT distributions are corrected for bin-migration effects arising from the detector resolution and from final state radiation (FSR) using an unfolding technique. The smearing of the muon momentum in the detector is estimated, from simulation, with a parametrized function derived from a double Gaussian fit. Additional scale factors are applied on the standard deviations of the two Gaussians in order to account for the disagreement in the data and the simulation by comparing the dimuon mass distribution for different regions of η and pT. The average scale factor is determined to be about 1.1 ± 0.1. The final result is normalized by the measured total cross section in the range of the Z boson $60 < M_{\mu\mu} < 120$ GeV.

Since the differential cross section is normalized by the total cross section near Z resonance, several sources of systematic uncertainty cancel out completely (e.g. the integrated luminosity), and some, only partially (e.g. the lepton efficiency). The leading sources of systematic uncertainty considered in the measurement of the normalized distribution are the estimates of the backgrounds, the determination of the ratio of the reconstruction and trigger efficiencies in data and MC, the construction of the response matrices to correct for the detector resolution and the FSR. For each of the systematic uncertainty, we recalculate the normalized qT distribution and take the maximum positive and negative differences in the obtained results of the normalized cross section with respect to the nominal one as the systematic uncertainty. The total systematic uncertainty in each bin is found to be smaller than the statistical uncertainty.

4.2 Results

Measurements of the qT distribution for the Z boson in hadron collisions provide an important test of the QCD predictions for the gluon radiation in the initial state.

Fig. 2 compares the normalized dimuon transverse-momentum distribution from data (points) with different theoretical predictions (curves). Comparisons have been made separately between the data and the predictions of POWHEG event generator interfaced with PYTHIA using Z2star tune for the underlying events, MADGRAPH event generator with the same Z2star tune for the hadronization with PYTHIA, and Resbos. The uncertainties associated with the data correspond to the statistical and systematic uncertainties summed in quadrature. The horizontal lines indicate the bin boundaries and the data points are positioned at the average of the bins. The lower portion of the figure shows the difference between the data and the simulation predictions divided by the uncertainty (statistical and systematic) on the data, σ_{data}. The green (inner) and yellow (outer) bands are the ranges corresponding to $\pm 1\sigma$ and $\pm 2\sigma$ experimental uncertainties.

MADGRAPH shows a better agreement throughout the observed qT range with respect to the predictions from POWHEG+PYTHIA. In particular, at high values of qT, MADGRAPH can reproduce better the data since it emulates multiple hard emissions which PYTHIA cannot do. The Resbos package adopted the Collins-Soper-Sterman formalism for the resummation of the multiple and collinear gluon emmissions [11], [12]. The predictions from Resbos are better than those achieved in other cases discussed earlier.

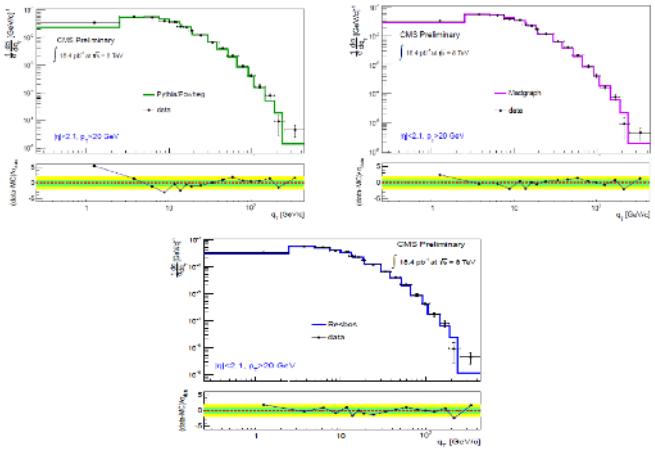

Figure 2. Comparison of the normalized dimuon transverse momentum distribution from data (points) with different theoretical predictions (curves) in the restricted detector acceptance.

5 Measurement of the differential and double-differential Drell-Yan cross sections at $\sqrt{s}$ = 7 TeV

5.1 Analysis strategy

The events in the dielectron channel are selected if triggered by two electrons with minimum E_T requirements 17 GeV for one of the electrons and 8 GeV for the other. Electrons are required to be isolated and to be within $|\eta| < 1.44$ or $1.57 < |\eta| < 2.5$, asking for the leading electron $pT >$ 20 GeV and for the sub-leading electron $pT > 10$ GeV.

The events in the dimuon channel are selected if triggered by two muons with minimum pT requirements 13 GeV for one of the muon and 8 GeV for the other. Muons are required to be isolated and to be within $|\eta| < 2.4$, asking for the leading muon $pT > 14$ GeV and for the sub-leading muon $pT > 9$ GeV.

Monte Carlo (MC) samples are used in the analysis for determining efficiencies, acceptances, backgrounds from processes that result in two leptons ($Z \to \tau\tau$, $t\bar{t}$, W + jets, diboson (WW, WZ and ZZ), and QCD), and for the determination of systematic errors. To match the observed instantaneous luminosity profile of the LHC, the simulated events are reweighted to yield the same distribution of the mean number of proton-proton interactions per bunch crossing as observed in data. Data driven methods are also used to determine efficiency correction factors and cross-check backgrounds estimation, using the $e\mu$ method described in section 4.

The measurements of energy and momentum of each lepton directly affect the reconstructed dilepton invariant mass and are critical in obtaining a correct differential cross section. Both for muons and electrons momentum-scale corrections are applied. The effects of the detector resolution and FSR in the migration of events among analysis bins is corrected through an unfolding procedure .The differential cross section measurements are normalized to the Z-peak region (60-120 GeV). In table 2 there is a summary of systematic uncertainties in the electron and muon channel (in percent). With the exception of "Acceptance", the numbers correspond to the individual measurements per bin and not the ratio to the Z region.

Table 2. Systematic uncertainties for e and μ channel (in percent). With the exception of "Acceptance", the numbers correspond to the individual measurements per bin and not the ratio to the Z region.

Invariant mass bin (GeV)	Energy Scale e	Efficiency correction e	μ	Background e	μ	Unfolding e	μ	FSR μ	Acceptance e	μ
15-20	23.4	9.2	1.1	6.2	3.6	8.7	0.4	1.5	+2.1/-2.9	+2.2/-3.0
20-30	3.6	8.5	1.1	2.8	3.1	2.1	0.2	1.1	+1.7/-2.8	+1.9/-3.2
30-40	2.7	9.4	1.2	4.0	1.9	1.5	0.1	0.7	+1.5/-2.7	+1.7/-3.0
40-50	3.3	7.5	1.2	5.2	1.7	1.4	0.2	0.7	+1.5/-2.5	+1.7/-2.9
50-60	3.3	5.2	0.8	4.6	2.1	1.9	0.2	0.5	+1.5/-2.4	+1.7/-2.8
60-76	10.3	3.3	0.6	2.2	1.0	2.0	0.2	1.4	+1.4/-2.3	+1.6/-2.6
76-86	39.5	2.5	0.4	0.8	0.2	3.1	1.7	2.0	+1.3/-2.2	+1.5/-2.5
86-96	3.9	1.9	0.3	0.2	0.05	0.6	0.2	0.5	+1.2/-2.1	+1.5/-2.4
96-106	45.6	2.0	0.3	0.9	0.4	3.6	3.8	0.5	+1.3/-2.0	+1.5/-2.4
106-120	13.2	2.1	0.3	2.6	1.4	2.4	0.7	0.5	+1.3/-1.9	+1.5/-2.3
120-150	6.0	2.4	1.1	8.2	2	2.6	0.4	0.5	+1.3/-1.8	+1.5/-2.1
150-200	5.7	2.8	2.1	12.9	6	2.4	0.9	0.5	+1.2/-1.5	+1.4/-1.8
200-600	4.6	3.2	2.1	11.8	10	1.6	0.1	0.5	+1.0/-1.1	+1.2/-1.4

5.2 Results

The result of the measurement of differential cross-section is in good agreement with the NNLO theoretical predictions as computed with FEWZ 2.1.1 (CT10 set of PDFs), and shown in fig. 3. The error band in fig. 3 for the theory calculation includes the statistical error from the FEWZ calculation and 68% CL PDF uncertainty combined in quadrature (blue band). The effect of the higher order EWK correction, including $\gamma\gamma$ initiated processes effect computed with FEWZ 3.1.b2, is considered as an additional systematic uncertainty (green band). Fig. 4 shows

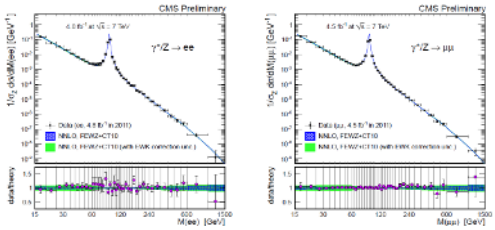

Figure 3. The Drell-Yan dielectron (left) and dimuon (right) invariant mass spectra, normalized to the Z-peak region, as measured and as predicted by FEWZ+CT10 NNLO calculations.

results of double differential cross-section against dimuon pseudorapidity for different bin of mass. The predictions of various existing PDF sets are rather different, especially in the low-mass region, high-mass and high-rapidity regions, while they are relatively close to each other and in good agreement with data in peak region. Given the uncertainties, the measurement presented provides sufficient sensitivity to different PDFs and can be used for new generation of PDFs. The error bands in the theory expectations in the figure indicate the statistical calculation error only from the FEWZ calculation.

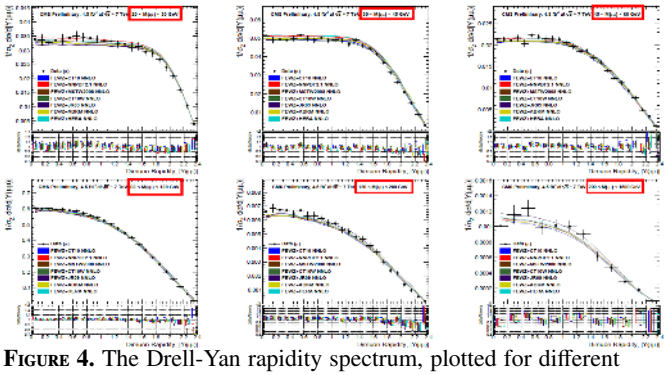

Figure 4. The Drell-Yan rapidity spectrum, plotted for different mass regions within the detector acceptance, normalized to the Z-peak region, as measuerad and predicted using various PDF sets.

6 Measurement of lepton charge asymmetry

6.1 Analysis strategy

For $W \to l\nu$ ($l = e, \mu$), the lepton charge asymmetry is defined as $A(\eta) = \frac{d\sigma/d\eta(W^+ \to l^+\nu) - d\sigma/d\eta(W^- \to l^-\bar{\nu})}{d\sigma/d\eta(W^+ \to l^+\nu) + d\sigma/d\eta(W^- \to l^-\bar{\nu})}$

In $W \to e\nu$, candidates were collected using a set of inclusive single-electron triggers and are required to have $|\eta| <$ 2.4 and pT > 35 GeV (where the trigger was fully efficient). Due to the substantial amount of material in front of the ECAL detector, a large fraction of electrons radiate photons. Photons may convert close to the original electron trajectory, leading to a sizable charge misidentification rate which dilute the true charge asymmetry. Differ-

ent methods are used to evaluate the charge of the electron. They are based on electron reconstruction algorithms and its trajectory and are required to give the same sign of charge. This procedure significantly reduces the charge misidentification rate to 0.1% in the ECAL barrel and to 0.4% in the ECAL endcaps. The events passing the above selection criteria are divided into six bins of electron pseudorapidity ($|\eta^e|$) : [0.0, 0.4], [0.4, 0.8], [0.8, 1.2], [1.2, 1.4], [1.6, 2.0], and [2.0, 2.4]. A binned extended maximum likelihood fit is performed over the E_T^{miss} distribution. The method is similar to the one used in section 3 to to estimate the $W \to e\nu$ signal yield for electrons (N^-) and positrons (N^+) in each pseudo-rapidity bin and to estimate QCD and other EWK backgrounds.

In $W \to \mu\nu$, candidates were collected using a set of inclusive single-muon triggers and are required to have $|\eta| <$ 2.1 and pT > 25 GeV. The muon candidate is not required in this analysis to be isolated from other event activity in order to avoid bias in the signal extraction fit described below. The muon charge misidentification rate is studied using $W \to \mu\nu$ MC simulations and is estimated to be at the level of 10^{-5}. The events which passed the above selection criteria are divided into six bins of muon pseudorapidity ($|\eta^\mu|$) : [0.0, 0.4], [0.4, 0.8], [0.8, 1.2], [1.2, 1.5], [1.5,1.8], and [1.8, 2.1]. The $W \to \mu\nu$ signal estimation is done by fitting the distribution of an isolation variable $\zeta = \sum(E_T)$, defined as the scalar sum of the transverse momenta of silicon tracks (excluding the muon candidate) and energy deposits in both ECAL and HCAL in a cone $\Delta R < 0.3$ around the muon direction. The shape of the ζ distribution for muons from $W \to \mu\nu$ is parametrized as a Landau distribution convolved with a Gaussian resolution function. An unbinned extended maximum likelihood fit to the ζ distribution is performed simultaneously on the $W^+ \to \mu^+\nu$ and $W^- \to \mu^-\bar{\nu}$ candidates to determine the total $W \to \mu\nu$ signal yield and the charge asymmetry in each pseudorapidity bin.

The main systematics are summarized in table 3

Table 3. Syst. uncert. for e and μ channel (in percent)

Ele channel							
η bin	Sig.& Bkg. Estim.		Eff. Ratio		En. scale and resol.		Charge Misid.
	e	μ	e	μ	e	μ	e
[0.00, 0.20]	1.8	0.22	4.5	0.25	0.6	0.25	<0.1
[0.20, 0.40]	2.5	0.23	4.4	0.26	0.6	0.25	<0.1
[0.40, 0.60]	2.7	0.25	4.4	0.25	0.3	0.25	<0.1
[0.60, 0.80]	2.5	0.28	4.4	0.26	0.3	0.25	<0.1
[0.80, 1.00]	1.9	0.33	4.4	0.29	0.6	0.25	0.1
[1.00, 1.20]	2.4	0.37	4.9	0.30	1.0	0.25	0.1
[1.20, 1.40]	2.6	0.42	5.4	0.32	0.8	0.25	0.1
[1.40, 1.60]	3.1	0.47	9.2	0.33	0.8	0.25	0.1
[1.60, 1.85]	2.0	0.49	8.7	0.33	1.6	0.25	0.2
[1.85, 2.10]	2.0	0.53	10.0	0.39	2.6	0.25	0.3
[2.10, 2.40]	2.9	0.58	12.5	1.10	2.4	0.85	0.3

6.2 Results

The experimental results for $W \to e\nu$ and $W \to \mu\nu$ are shown in fig. 5. Comparison is done with theoretical predictions obtained with the NLO MCFM generator interfaced with CT10, HERAPDF, NNPDF, and MSTW2008NLO PDF models. For $W \to e\nu$ the experimental data are in agreement with the predictions from CT10, NNPDF, and HERAPDF, while the predictions from MSTW are systematically lower than the observed asymmetry in the region $|\eta| < 1.4$. For $W \to \mu\nu$ data exhibit a flatter variation of the asymmetry with pseudorapidity than predicted by the MSTW2008NLO, CT10W, and NNPDF2.1 (NLO) PDF sets.

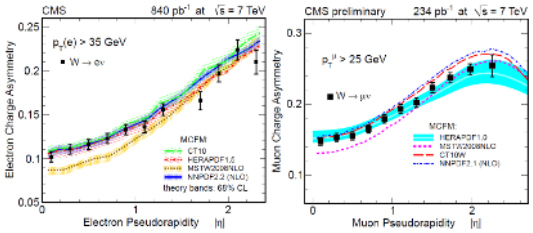

Figure 5. Comparison of the measured lepton charge asymmetry to different PDF models for e channel (left) and μ channel (right).

References

[1] C. Anastasiou, L. Dixon, and F. Petriello, "High precision QCD at hadron colliders :Electroweak gauge boson rapidity distributions at NNLO", *Phys. Rev. D* **69** (2004) 094008, *doi :10.1103/PhysRevD.69.094008*.

[2] K. Melnikov and F. Petriello, "Electroweak gauge boson production at hadron colliders through O(α_s^2)", *Phys. Rev. D* **74** (2006) 114017, *doi :10.1103/PhysRevD.74.114017*.

[3] CMS Collaboration, "Inclusive W/Z cross section at 8 TeV", *CMS-PAS-SMP-12-011 - https ://cdsweb.cern.ch/record/1460098*.

[4] CMS Collaboration, "Measurement of the transverse momentum distributions of Z Bosons decaying to dimuons in pp collisions at $\sqrt{s}$=8 TeV", *CMS-PAS-SMP-12-025 - https ://cdsweb.cern.ch/record/1528579*

[5] CMS Collaboration, "Measurement of the differential and double-differential Drell-Yan cross section in proton-proton collisions at 7 TeV" *CMS-PAS-SMP-13-003 - https ://cdsweb.cern.ch/record/1543468*

[6] CMS Collaboration, "Measurement of the Electron Charge Asymmetry in Inclusive W Production in pp Collisions at $\sqrt{s}$=7 TeV" *Phys. Rev. Lett.* **109** (2012) 111806 *10.1103/PhysRevLett.109.111806*

[7] CMS Collaboration, "Measurement of the muon charge asymmetry in inclusive W production in pp collisions at $\sqrt{(s)}$=7 TeV" *CMS-PAS-EWK-11-005 - https ://cdsweb.cern.ch/record/1377410*

[8] CMS Collaboration, "The CMS Experiment at the CERN LHC", *JINST* **0803** (2008) S08004, *doi :10.1088/1748-0221/3/08/S08004*.

[9] CMS Collaboration, "Electron reconstruction and identification at $\sqrt{s}$= 7 TeV" *Physics Analysis Summary EGM-10-004* 2010 .

[10] CMS Collaboration, "Performance of muon identification in pp collisions at $\sqrt{s}$= 7 TeV" *CMS Physics Analysis Summary MUO-10-002* 2010 .

[11] J. C. Collins and D. E. Soper, "Back-To-Back Jets in QCD", *Nucl.Phys.* **B193** (1981) 381, *doi :10.1016/0550-3213(81)90339-4*.

[12] J. C. Collins, D. E. Soper, and G. F. Sterman, "Transverse Momentum Distribution in Drell-Yan Pair and W and Z Boson Production", *Nucl.Phys.* **B250** (1985) 199, *doi :10.1016/0550-3213(85)90479-1*.

[13] V. Blobel, "An unfolding method for high-energy physics experiments", *arXiv :hep-ex/0208022*.